A DYNAMICAL MODEL FOR PULSATILE FLOW ESTIMATION IN A LEFT VENTRICULAR ASSIST DEVICE

Abdul-Hakeem H. AlOmari, Andrey V. Savkin

School of Electrical Engineering and Telecommunications, The University of New South Wales, Sydney, Australia

Dean M. Karantonis[§], Einly Lim[†] and Nigel H. Lovell[†]

[§]*Ventracor Limited;*[†]*Graduate School of Biomedical Engineering, The University of New South Wales, Sydney, Australia*

Abstract: In this paper, we propose a dynamical model for pulsatile flow estimation of an iRBP. Noninvasive measurements of the motor power (VI) and pump impeller rotational speed (ω) were acquired from the pump controller and used together with blood hematocrit (HCT) values as inputs to the model. A circulatory mock loop was operated with different aqueous glycerol solutions, mimicking different values of viscosities equivalent to the range of 20 - 50% of human blood HCT, to generate pulsatile flow data. Linear regression between estimated pulsatile flow (Q_{est}) and measured flow (Q_{meas}) obtained from the mock loop resulted in a highly significant correlation ($R^2 = 0.957$) and mean absolute error of $e = 0.364$ L/min. Also, $R^2 = 0.902$ and $e = 0.317$ L/min were obtained when our model was validated using six sets of *ex vivo* porcine data. Furthermore, in steady state, the solution of the presented model can be described by a previously designed and verified static model.

1 INTRODUCTION

The problem of noninvasive estimation of flow rate has attracted the attention of many research groups (for examples, see (Bertram, 2005)). It has been shown that flow rate can be accurately estimated under steady-state conditions (Malagutti et al., 2007; Ayre et al., 2003; Funakubo et al., 2002; Kitamura et al., 2000; Tsukiya et al., 2001).

Pulsatile flow estimation of iRBPs has been much less frequently studied. This may be due to the large number of factors that need to be taken into consideration. Such factors may include the use of characteristics curves of the pump where these are sensitive to many physiological and mechanical parameters like: changing blood viscosity, impeller inertia of the pump.

In the present study, we used noninvasive feedback measurements of ω and VI to estimate the pulsatile pump flow using a new dynamical model. When operated in steady state conditions, our model can provide an accurate estimate of the flow which agrees with those obtained from the static model developed in our laboratory under non-pulsatile conditions in

Malagutti et al. (2007). Another practically important requirement for our dynamical model is its stability. The proposed model will allow us to accurately study and estimate the transient response and the dynamics of the pulsatile flow.

2 MATERIALS AND METHODS

2.1 *In vitro* Pulsatile Experiments

A VentrAssist^{TM} (Ventracor Limited, Sydney, Australia) iRBP was connected in a circulatory mock loop in a pulsatile environment. The loop was composed of venous and arterial reservoir tanks, a silicone bag which represented the left ventricle chamber (Karantonis et al., 2007). Ventricular contraction was simulated by periodically compressing the mock ventricle with pneumatic pistons at a fixed rate. Arterial pressure, central venous pressure, pump inlet and outlet pressure were measured. Pulsatile flow was measured by an Ultrasonic flow probe (Transonics Systems Inc., Ithaca, NY, USA). The instantaneous ω, motor volt-

age and current were accessed as feedback signals from the controller. Speed was varied from 1800 to 3000 rpm in a stepwise increment of 100 rpm lasting for 30 s. For each step, systemic resistance was also changed to cover the range of desired flows. The sampling rate was 4 kHz for data recordings, but, in further analysis, the data were down-sampled to 50 Hz.

2.2 *Ex vivo* Animals Experiments

The VentrAssist^{TM} was acutely implanted in six healthy pigs. In each pig, the inflow pump cannula was inserted into the apex of the left ventricle while the outflow cannula was anastomosed to the ascending aorta (Karantonis et al., 2006). Indwelling catheters (DwellCath, Tuta Labs, Lane Cove, NSW, Australia) and pressure transducers (Datex-Ohmeda, Homebush, NSW, Australia) were instrumented to the pig's native heart to measure left ventricle, left atrial, aortic, and pump inlet pressures. Pump and aortic flows were measured by ultrasonic flow probes from the outlet cannula of the pump. Besides these signals, the noninvasive ω, motor current (I), and supply voltage (V) were acquired from the pump controller. The experimental data were sampled at 200 Hz. For further information about data acquisition, see Karantonis et al. (2006).

2.3 Dynamical Modeling

2.3.1 Static Flow Model

A noninvasive, steady-state average flow (Q_{ss}) estimator was designed in a non-pulsatile environment for the iRBP. The estimator was based on VI, and ω. The static equation for the flow estimator is based on the work of Malagutti et al. (2007) and Ayre et al. (2003) and is of the following form:

$$Q_{ss} = a + bVI + cVI^2 + dVI^3 + e\omega + p\omega^2, \quad (1)$$

where a, e, and p, are constants and the power coefficients b, c, and d were found to have a linear relationship with the HCT (Malagutti et al., 2007).

2.3.2 Pulsatile Flow

In this section, we describe a dynamical model for the iRBP. The main requirement for the dynamical model is that any steady-state solution of the dynamical model be a solution of the static equation (1). Furthermore, we want any steady-state solution of the dynamical model to be stable. We introduce a variable $f(t)$ as follows:

$$f(t) = g(VI(t), \omega(t)), \quad (2)$$

where

$$g(VI(t), \omega(t)) = a + bVI(t) + cVI^2(t) + dVI^3(t)$$
$$+ e\omega(t) + p\omega^2(t). \quad (3)$$

Here $t = kh$, $h > 0$ is the sampling interval, $k = 0, 1, 2, 3, \ldots$. In other words, the variable $f(t)$ represents the right-hand side of the static equation (1), describing the pump flow in steady-state. We introduce a dynamical model of the form:

$$(A(\nabla) + B(\nabla))Q_{est}(t) = B(\nabla)f(t), \quad (4)$$

where $Q_{est}(t)$ is the output of the system which represents the estimated instantaneous values of the pulsatile flow ($Q(t)$), $f(t)$ is the input to the dynamical system model, ∇ is the shift operator, $A(\nabla)$, $B(\nabla)$ are polynomials defined as follows:

$$A(\nabla)Q_{est}(t) = \sum_{i=0}^{n} a_i Q_{est}(t - i + 1), \quad (5)$$

$$B(\nabla)f(t) = \sum_{j=1}^{m} b_j f(t - j + 1). \quad (6)$$

Here n is the model output order, and m is the model input order satisfying the condition $m \leq n$.

Now we describe all steady-state or constant solutions of the equation (3). Let $Q_{est}(t) \equiv Q_0$ and $f(t) \equiv f_0$ for all $t = 0, 1, 2 \ldots$, then, we obtain from (4) that

$$(A(1) + B(1))Q_0 = B(1)f_0. \quad (7)$$

We assume that $A(1) = 0$ and $B(1) \neq 0$. This yields to the following conditions on parameters coefficients of the model:

$$\sum_{i=0}^{n} a_i = 0, \quad (8)$$

$$\sum_{j=1}^{m} b_j \neq 0. \quad (9)$$

Under the assumptions (8) and (9), it immediately follows from (7) that

$$Q_0 = f_0. \quad (10)$$

Since $f(t)$ is defined by (2), (3), (10) it implies that Q_0 is the corresponding solution of the equation (1). Hence, steady-states of the dynamical model are described by the static model.

Furthermore, if the system is stable i.e; all z : $A(z) + B(z) = 0$ belong to $|z| < 1$ (all poles of the system are inside the unit disk) (Ogata, 1995), then the solution of the dynamical system (4) with any initial conditions and with a constant input f_0 will converge to the constant output Q_0 satisfying (10).

2.3.3 Data Analysis

Data was divided into two sets, one set was used for identification and training and the other to validate the model. The off-line least squares method (Ljung, 1999) was used to estimate the model coefficients. Values of parameter coefficients were chosen so that the error between estimated $Q_{est}(t)$ and measured flow $Q_{meas}(t)$ was minimized. Also, parameters should fulfill the assumptions defined in equations (8) and (9). Mean absolute error (e), and correlation coefficient (r) were used to check the performance of the model as follows:

$$e = \frac{1}{N} \sum_{i=1}^{N} (Q_{meas}(t) - Q_{est}(t))^2, \qquad (11)$$

$$r = \frac{\sum_{i=1}^{N} (Q_{meas}(t) - \overline{Q_{meas}})(Q_{est}(t) - \overline{Q_{est}})}{\sqrt{\sum_{i=1}^{N} (Q_{meas}(t) - \overline{Q_{meas}})^2 \sum_{i=1}^{N} (Q_{est}(t) - \overline{Q_{est}})^2}}. \qquad (12)$$

Here N is the length of data. $\overline{Q_{meas}}$, and $\overline{Q_{est}}$ are the mean values of the measured and estimated flows respectively.

3 RESULTS

Least e and highest r between the estimated and measured flow in both mock loop and animal experiments were obtained with system model orders of $n = 3$ and $m = 2$. The resulting model is described as follows:

$$a_0 Q_{est}(t) + (a_1 + b_1)Q_{est}(t-1) + (a_2 + b_2)Q_{est}(t-2)$$
$$+ a_3 Q_{est}(t-3) = b_1 f(t-1) + b_2 f(t-2), \qquad (13)$$

where $a_0 = 1$, $a_1 = -2.25$, $a_2 = 1.49$, $a_3 = -0.24$, $b_1 = 0.27$, $b_2 = -0.25$, Q_{est} is the estimated pulsatile flow, and $f(t)$ is the input signal. The poles-zeros plot of the system shown in figure 1 demonstrates that the model is stable. The dashed line in figure 2 shows part of the estimated pulsatile and measured flow obtained from the mock loop.

Linear regression analysis between $Q_{est}(t)$ and $Q_{meas}(t)$ obtained from the mock loop experiments is illustrated in figure 3. A highly significant correlation between estimated and measured flow was obtained with a small mean absolute error value.

During animal experimentation the values of HCT were not measured. Instead, for each animal we used the values of HCT that gave the best fit between the estimated and measured flows in the steady state model described in equation (1). Additionally, two sets of data were removed from the analysis due to
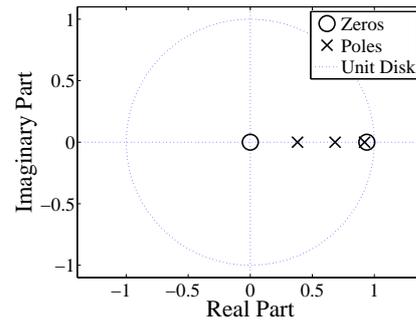
Figure 1: Poles-zeros plot of the system model described by equation (13).
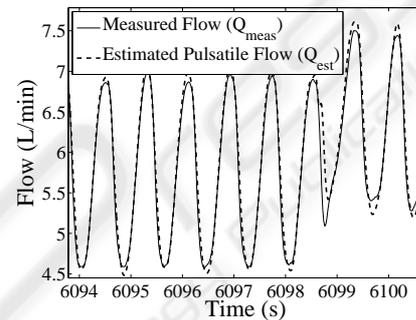
Figure 2: Estimated pulsatile flow compared with measured flow obtained from mock loop.
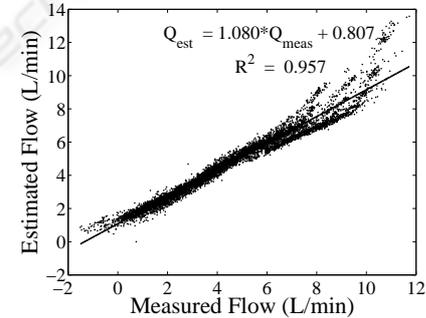
Figure 3: Linear regression plot between estimated versus measured flow obtained from mock loop.

excessively noisy power signals. The comparison between estimated pulsatile and real flow for one of the six animal experiments is shown in figure 4. Correlation between estimated and real flows was highly significant ($R^2 = 0.902$), with small mean absolute error $e = 0.317$ L/min.

The response of the proposed model to abnormal flow conditions associated with different pumping states such as ventricular collapse (VC) and aortic valve not opening (ANO) were accurately estimated by the model (not shown).
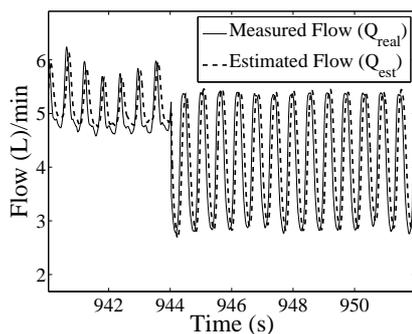
Figure 4: Estimated flow compared with measured one obtained from pigs experiments.

4 DISCUSSION

In the present study, a dynamical model for pulsatile flow estimation was successfully designed. In the proposed model, the level of *HCT* was assumed to be known. This is the major limitation of the presented model.

Using an autoregressive with exogenous input (ARX) model, Yoshizawa et al. (2002) developed a pulsatile flow estimator (Yoshizawa et al., 2002). A Mean absolute error of 1.66 L/min, and a correlation coefficient of 0.85 were obtained when another ARX model has used to compensate for *HCT*. Tsukiya et al. (2001) showed that the non-pulsatile flow rate estimator was able to monitor the instantaneous flow (Tsukiya et al., 2001). To compare, our proposed model resulted in a high correlation coefficient R^2= 0.957 with e= 0.364 L/min in mock loop. Also R^2= 0.902 and e= 0.317 L/min were obtained using *ex vivo* animals data.

Ayre et al. (2003) were successfully estimated an average flow for non-pulsatile and pulsatile flow (Ayre et al., 2003). More recently, pulsatile flow was accurately estimated by Karantonis et al. (2007). Although these studies produced acceptable results, they did not study the stability of the transient response of the pump flow which is one of the outcomes of the present study.

5 CONCLUSIONS

A dynamical model for an iRBP has been presented and shown to accurately estimate the pulsatile flow using noninvasive measurements of power and speed. Furthermore, the proposed model is stable and its set of steady states is identical to the set of solutions of the previously derived static model.

ACKNOWLEDGEMENTS

REFERENCES

Ayre, P. J., Lovell, N. H., and Woodard, J. C. (2003). Non-invasive flow estimation in an implantable rotary blood pump: a study considering non-pulsatile and pulsatile flow. *Physiol Meas*, 24:179–89.

Bertram, C. (2005). Measurement for implantable rotary blood pumps. *Physiol Meas*, 26:R99–R117.

Funakubo, A., Ahmed, S., Sakuma, I., and Fukui, Y. (2002). Flow rate and pressure head estimation in a centrifugal blood pump. *Artif Organs*, 26:985–90.

Karantonis, D. M., Cloherty, S. L., Mason, D. G., Ayre, P. J., and Lovell, N. H. (2007). Noninvasive pulsatile flow estimation for an implantable rotary blood pump. In *Proceedings of the 29th Annual International Conference of the IEEE EMBS*.

Karantonis, D. M., Lovell, N. H., Ayre, P. J., Mason, D. G., and Cloherty, S. L. (2006). Identification and classification of physiologically significant pumping states in an implantable rotary blood pump. *Artif Organs*, 30:671–9.

Kitamura, T., Matsushima, Y., Kono, S., Nishimura, K., Komeda, M., Yanai, M., Kijima, T., and Nojiri, C. (2000). Physical model-based indirect measurements of blood pressure and flow using a centrifugal pump. *Artif Organs*, 24:589–93.

Ljung, L. (1999). *System Identification: Theory for the user*. Prentice Hall PTR, USA, 2nd edition.

Malagutti, N., Karantonis, D. M., Cloherty, S. L., Ayre, P. J., Mason, D. G., Salamonsen, R. F., and Lovell, N. H. (2007). Noninvasive average flow estimation for an implantable rotary blood pump: a new algorithm incorporating the role of blood viscosity. *Artif Organs*, 31:45–52.

Ogata, K. (1995). *Discrete-Time Control Systems*. Prentice Hall Inc., USA, 2nd edition.

Tsukiya, T., Taenaka, Y., Nishinaka, T., Oshikawa, M., Ohnishi, H., Tatsumi, E., Takano, H., Konishi, Y., Ito, K., and Shimada, M. (2001). Application of indirect flow rate measurement using motor driving signals to a centrifugal blood pump with an integrated motor. *Artif Organs*, 25:692–96.

Yoshizawa, M., Sato, T., Tanaka, A., Abe, K., Takeda, H., Yambe, T., Nitta, S., and Nose, Y. (2002). Sensorless estimation of pressure head and flow of a continuous flow artificial heart based on input power and rotational speed. *ASAIO Journal*, 48:443–48.